ASME 2012 5th Annual Dynamic Systems and Control Conference joint with the JSME 2012 11th Motion and Vibration Conference
DSCC2012-MOVIC2012
October 17-19, 2012, Fort Lauderdale, Florida, USA

DSCC2012-MOVIC2012-8757

HIGH-BANDWIDTH SCANNING OF SAMPLE PROPERTIES IN ATOMIC FORCE MICROSCOPY

Gayathri Mohan
Dept. of Mechanical Science and Engg.
University of Illinois, Urbana-Champaign
Urbana, Illinois 61801
Email: gmohan2@illinois.edu

Chibum Lee
Dept. of Mechanical System Design Engg.
Seoul National University of Science and Technology
Seoul, Korea 139-743
Email:chibum@seoultech.ac.kr

Srinivasa M Salapaka *
Email: salapaka@illinois.edu

ABSTRACT

This paper exemplifies methods to estimate sample properties, including topographical properties, from a high bandwidth estimate of tip-sample interaction forces between the probe tip and the sample surface in an atomic force microscope. The tip-sample interaction force is the most fundamental quantity that can be detected by the probe tip. The fact that sample features as well as physical properties of the sample are a function of tip-sample interaction model chosen is exploited, and the property estimates are obtained by fitting appropriate physical models to the force estimate data. The underlying idea is to treat the nonlinear tip-sample interactions as a disturbance to the cantilever subsystem and design a feedback controller that ensures the cantilever deflection tracks a desired trajectory. This tracking allows scanning speeds as high as $\frac{1}{10}^{th}$ of the cantilever resonance frequency compared to typical scanning modes that regulate derivatives of the probe deflection such as amplitude or phase, providing much lower scan speeds. The high bandwidth disturbance rejection and consequent estimation provides estimates of the tip-sample interaction force.

1 INTRODUCTION

The atomic force microscope (AFM) is a powerful scanning probe device that facilitates study of sample surfaces at nano scales [1]. The ability of the cantilever to detect forces in the order of $1-100$ pN is used to obtain high resolution images of sample topography. This is carried out by recording, or regulating in closed-loop operation, the changes in the cantilever behavior such as its deflection, amplitude or phase due to tip-sample interaction forces. Figure 1(a) depicts the basic operating principle of an AFM. The two common modes of operation in an AFM are (i) *Contact or static mode:* the cantilever deflection is maintained constant by changing the piezo-actuation signal in the z or vertical direction using feedback to compensate for sample features across a raster scan, (ii) *Tapping or dynamic mode:* the cantilever is oscillated near or at its resonance frequency and the amplitude of oscillation is maintained constant using the z piezo-actuation signal. The interaction forces between the tip and the sample in a typical AFM are predominantly nonlinear functions of the tip-sample separation distance and their physical properties. Subsequently, the regulating actuation signal serves as a measure of the sample topography in both modes. In addition to measuring the sample's topographical features, the ability of AFM to measure forces in the order of pico-Newtons facilitates the measurement of sample properties from the corresponding forces.

In most commercial AFM systems, lateral positioning bandwidths are about one percent of resonant frequencies of the cantilevers ($1-3$ kHz vs $100-300$ kHz), and therefore the cantilever does not encounter appreciable difference in sample surface over a few cycles of oscillation. The amplitude-regulating control effort can thus be reliably used as a sample height measure . However, regulation of the "slow" amplitude signal which is a derivative of the cantilever deflection cannot exploit the recent advances in high-bandwidth nanopositioners providing speeds of 10%-20% of the cantilever resonant frequencies [2–4]. In [5], the emergence of high-bandwidth positioners and faster electronics are taken into account and a high-speed dynamic

*Affiliation same as first author

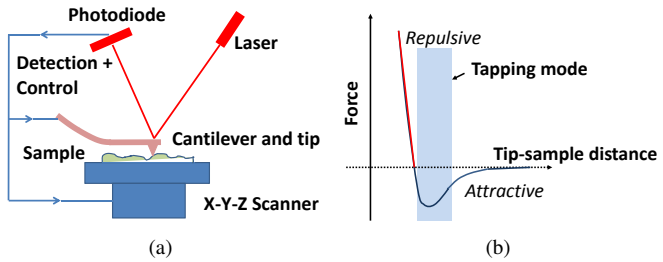

Figure 1. (a) The change in cantilever deflection is recorded by means of a laser mirror arrangement, that reflects a laser beam off of the cantilever tip on to a photodiode. In closed-loop operation, this signal may be used in feedback for regulation of relevant parameters (b) The force curve shows the attractive and repulsive zones of interaction as a function of the tip-sample separation.

imaging mode is proposed that overcomes the bandwidth limitations while preserving the advantages of high resolution and gentle contact on the sample provided by the dynamic mode. The key idea was to treat the nonlinear tip-sample interaction force as an exogenous disturbance to a linear cantilever subsystem. Rejection and estimation of the disturbance signal through control techniques renders estimates of interaction forces. The tip-sample interaction force estimate in comprehensive in the sense that it contains information about the sample's topographical as well as physical properties such as stiffness. The objective of this paper is to address the estimation of sample properties from the high-bandwidth tip-sample interaction force estimates.

Force curves, which are plots of the interaction force against the tip-sample separation are used to obtain property estimates of the sample. Force modulation techniques were developed for samples with variations in local surface elasticity [6]. The variation in elasticity is measured by the changes in cantilever deflection under constant average force. In [7], the authors use a series of approach-retract force curves to obtain time series data of the cantilever response and thereby identify the cantilever transfer function. Here, small oscillation amplitudes are considered and the nonlinear tip-sample interaction force is assumed to be linearized and absorbed as a system internal parameter. Experiments in low damping environments have also been used to estimate the relationship between the cantilever frequency shift and the interaction potential [8]. Majority of these techniques utilize force curves taken at discrete locations on the sample quiasistatically and map them to physical properties. Although they are effective in estimating sample properties, they suffer from the disadvantages of long process time and limitations in the spatial/lateral resolution of the sample properties. Some other techniques like the contact-resonance AFM [9] estimate the viscoelastic properties of the sample without estimating the interaction forces, assuming a spring-dashpot tip-sample interaction model. The excitation of the cantilever at two frequencies (close to its natural frequency) in addition to oscillating it at resonance in tapping mode has been shown to estimate equivalent cantilever parameters at higher speeds than conventional techniques [10]. However, a simple model is assumed for the tip-sample interaction.

In this paper, a few potential methods to estimate sample properties from the high-bandwidth force estimates in [5] are outlined by means of examples. Section 2 gives a brief overview of force curves in AFM and physical models used to represent tip-sample interactions. Section 3 presents the design of control for force regulation and estimation, proposed in [5]. Section 4 exemplifies some methods to estimate sample properties from the interaction force estimates.

2 TIP-SAMPLE INTERACTION FORCES IN AFM

Typically, when the probe-sample separation is large the probe does not experience any short range forces and therefore there is no deflection detected. However, when the tip gets closer to the sample, the short range Van Der Waal forces act first as an attractive force that pulls the cantilever towards the sample surface. This may cause the cantilever to jump to contact. As the separation distance decreases further, the force becomes repulsive in nature (see Fig. 1(a)). The tip-sample interaction forces are the most fundamental quantities that the probe tip can detect. For instance, while scanning a compliant sample, although the probe is sensitive to any short range force coming from the sample, at a given location it cannot distinguish between the forces occurring due to sample features and those occurring due to the compliance of the sample. This division is completely determined by the physical model assumed for the tip-sample interaction forces.

The classical Hertz contact model accounts for elastic deformation of bodies under imposed loads during contact, however, it ignores forces of adhesion. The later force models in literature [11–13] have developed upon Hertz model by including adhesive forces or Van Der Waals forces. Such models are used extensively in AFM applications to model the tip-sample interaction force. Based on the nature of the probe tip and sample, appropriate models are chosen. For instance, for tips with small radius of curvature and high stiffness the DMT model is chosen. The DMT model considers the action of Van Der Waals along the perimeter of contact between the tip and the sample.

In our formulation we adopt a generic form for the tip-sample interaction force in the attractive and repulsive regions,

$$F_{ts}(z_s) = \begin{cases} \alpha(a_0 - z_s)^m & z_s < 0 \\ \beta + \gamma(z_s)^n & z_s \geq 0 \end{cases}, \qquad (1)$$

where α, β and γ are parameters governed by the properties of the interacting materials, and $z_s = a_0 - z$, with a_0 being the intermolecular distance and z is the separation between probe-tip and sample. For instance, in case of the DMT model widely used in AFM literature, $\alpha = \frac{-HR}{6}$, $\beta = \frac{-HR}{6a_0^2}$, $\gamma = \frac{4}{3}E\sqrt{R}$, and $m = -2$ and $n = 3/2$. Here, H denotes the material dependent constant,

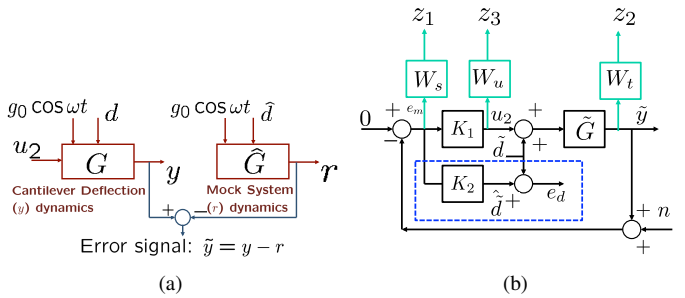

Figure 2. (a) G and $\hat{G}$ represent the real and the virtual mock system respectively. The objective of force regulation is realized by regulating the error between y the cantilever deflection and the reference r to zero (b) The error dynamics $\tilde{p}$ are represented by the block $\tilde{G}$. The controller K_1 designs the dither signal u_2 to reject disturbance $\tilde{d}$ that contains the nonlinear tip-sample interaction force terms. K_1 regulates the error between the real and the mock systems to zero. Furthermore, K_2 is designed to get an estimate ($\hat{\tilde{d}}$) of the disturbance $\tilde{d}$.

the Hamaker's constant, R is the tip radius, and E represents the effective Young's modulus between the tip and sample.

3 FORCE ESTIMATION

The force estimate obtained in [5] forms the basis for the sample property estimation, which is the primary focus in this work. Therefore, for completeness we provide a brief outline of our system model and the control design involved to eventually obtain the tip-sample interaction force estimate. Our setup considers the AFM cantilever dynamics modeled as a spring-mass-damper system as shown in [5]. In our model, the nonlinear tip-sample interaction force, modeled as the disturbance d, sinusoidal input $g_0 \cos \omega t$ oscillating the cantilever at a frequency ω close to its natural frequency ω_n and u_2, the control signal comprising of a fast component (to the dither piezo located at the base of the cantilever) and a slower component (to the z or vertical piezo) comprise the external inputs to the cantilever subsystem (see Fig. 2(a)). Force regulation is achieved by making the fast cantilever deflection signal follow a desired trajectory. The reference trajectory is generated by deploying a virtual mock system that is the cantilever subsystem tapping on an idealized flat sample surface. The interaction forces between the sample and the tip in the mock system are modeled by $\hat{d}$, shown in Fig. 2(a) using the DMT model [12]. It must be noted that the mock system is solely used to derive a reasonable trajectory that aids in maintaining a constant force between the tip and sample surface. This ensures that the tip does not crash into or get disengaged from the sample surface. As a consequence, in the proposed method there is no requirement for the model used to generate $\hat{d}$ to be an accurate description of the actual tip-sample interaction d.

The error between the cantilever deflection of real and mock systems $p - \hat{p}$, denoted by $\tilde{p}$ follows,

$$\begin{aligned} \dot{\tilde{p}} &= A\tilde{p} + B(u_2 + \tilde{d}), \quad \tilde{p}(0) = p_0 - \hat{p}_0 \\ \tilde{y} &= C\tilde{p} + n, \end{aligned} \tag{2}$$

where A, B and C are state-space system matrices for the cantilever subsystem as shown in [5]. The disturbance $\tilde{d}$ represents the nonlinear forces coming from $d - \hat{d}$ and n is the measurement noise. Our objective is to regulate the deflection error $\tilde{y}$ to zero by rejecting the effect of disturbance $\tilde{d}$. This ensures force regulation and estimating $\tilde{d}$ is equivalent to estimating d because $\hat{d}$ is generated virtually and known to us. As shown in Fig. 2(b) the controller K_1 is designed for disturbance rejection, noise attenuation, low input energy to the controller and robust stability. Minimizing the $\mathscr{H}_\infty$ norm of the entire closed-loop transfer function from the exogenous inputs to the regulated outputs z_1, z_2 and z_3 limits the set of feasible K_1. Therefore, we pose a multi-objective optimization problem $\min_{K_1 \in \mathbf{K}} \gamma \left\| W_s \tilde{G} S \right\|_\infty + \left\| \begin{matrix} W_s S \\ W_t T \\ W_u K_1 S \end{matrix} \right\|_\infty$ where γ determines the relative importance between the two terms. $W_s \tilde{G} S$ and $W_s S$ are the closed-loop transfer functions from the disturbance and noise to the regulated error z_1. Appropriate design of W_s and minimization of these transfer functions improve the bandwidth of disturbance rejection making $S = 1/(1 + \tilde{G} K_1)$ small in wide range of frequencies. Most disturbances encountered by the cantilever subsystem including the tip-sample interaction forces in this model, fall within the disturbance rejection bandwidth of $15 - 20\%$ of the cantilever resonance frequency. Minimizing $W_t T$ guarantees noise attenuation because it is the transfer function from the noise to the regulated output z_2. W_t is shaped such that the complementary sensitivity function T has a small roll-off frequency and high roll-off rates imposing high resolution and noise attenuation. The optimization cost function also minimizes $W_u K_1 S$ imposing a low control effort. Furthermore, the weighting function W_s is also designed to keep the peak value of $||S||_\infty$ less than 2. This imposes robustness to uncertainties which may include other disturbances that are not included in the system model. Details of the control design and solution using linear matrix inequalities can be found in [5].

The controller K_2 is designed such that the error between the disturbance $\tilde{d}$ to the error system and its estimate $\hat{\tilde{d}}$ is zero with respect to $\tilde{d}$. The error in estimation is given by

$$\tilde{d} - \hat{\tilde{d}} = (1 - K_2 \tilde{G} S)\tilde{d} + K_2 S n. \tag{3}$$

Therefore, K_2 is designed as $S^{-1}\tilde{G}^{-1}\Psi_h$, where Ψ_h is a filter with cut-off frequency higher than the cantilever resonance frequency used to make the transfer function proper. As a result, irrespective of the K_1 design, K_2 guarantees the best estimate of $\tilde{d}$ since it makes the error in terms of the disturbance become zero. The robustness of the estimate is attributed to the sensitivity function S, which is already shaped for robustness objectives in our framework.

4 TOPOGRAPHY AND PROPERTY ESTIMATION

Please note that all plots contain non-dimensionalized values unless otherwise specified on their axes. In our simulations, a cantilever of natural frequency $\omega_n = 69.578$kHz, damping co-efficient $\xi = 0.0033$ and mass $m = 7.482 \times 10^{-12}$kg is considered. Frequency $\bar{\omega} = \omega_n$ and dither oscillation amplitude $b = 2.916$nm are used as normalization parameters wherever appropriate. The interpretation of sample properties and topography from the interaction force estimates are significantly dependent on the physical interaction model chosen. In [5], sample topography estimates are obtained with the assumption of DMT model on the forces. The difference between the forces in the real and the mock system $(d - \hat{d})$ is approximated by $\Theta(\tilde{y} - h)$, where Θ is the averaged slope of the force with respect to deflection error over each cycle of cantilever oscillation. Using enough data points the unknowns, Θ and h, the sample height profile are fit numerically. In this section, we pose a few scenarios as examples where we assume knowledge of one or more of the parameters involved in the generic interaction force model in (1) and propose schemes to fit the other unknowns. In the following discussion, the deflection (measured), also denoted by, p_1 and the force estimate $\hat{F}$, which is $\hat{\tilde{d}} + \hat{d}$ are always assumed to be known. Ideally, the force curve is a plot of the interaction forces

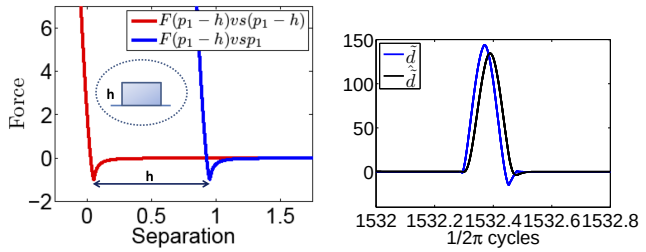

(a) (b)

Figure 3. (a) The displacement of the alternate force curve against cantilever deflection from the actual force-displacement curve provides an estimate of the sample height (b) The plot of the estimate $\hat{\tilde{d}}$ compared to original interaction force difference $\tilde{d}$ is shown. The estimate is able to capture the repulsive force region well although with a phase lag. However, the attractive region is not captured well enough for a h of frequency equal to 10% of the cantilever resonance frequency.

against the separation between the probe and sample surface, that is $F(p_1 - h)$ vs $(p_1 - h)$. However, the probe-sample separation $p_1 - h$ is not known since sample profile h is unknown. In our first attempt, we try to derive the properties of force-curve by analyzing the plot of force estimate $\hat{F}(p_1 - h)$ vs the cantilever deflection p_1 (see Figure 3(a)).

(i) Note that the estimated force-curve plot $F(p_1 - h)$ vs $p_1 - h$ is a translated version of the force-estimate vs deflection plot $\hat{F}(p_1 - h)$ vs p_1. A high bandwidth estimate of the interaction forces facilitates the estimation of sample topography by looking at the translated plots and averaging the translation over each or a few cantilever oscillation cycles where the sample profile h is approximately a constant. In typical force models as seen in Section 2, the repulsive tip-sample interaction force, denoted here by F_{ts} is given by,

$$F_{ts} = \beta + \gamma(z_s)^n, \tag{4}$$

where β and γ are parameters governed by the properties of the interacting materials, and z_s is a measure of separation between tip and sample. The repulsive forces are estimated well by the K_2 design as shown in Fig.3(b)

(ii) The slope of the repulsive force can be estimated using the force estimate data, by plotting it against the deflection values measured (Fig. 5(a)). The slope estimates over each cantilever oscillation cycle can provide dynamic estimates of the sample stiffness across a scan.

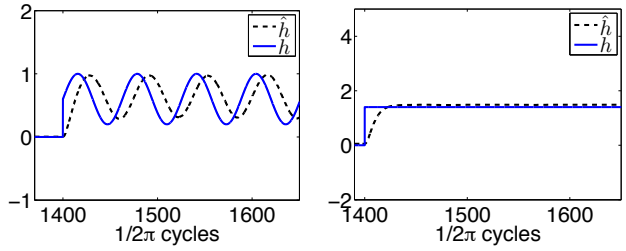

(a) (b)

Figure 4. (a) and (b) show the estimates through the topography estimation in [5] for completeness. The blue lines indicate the sample profile considered while the dotted lines show the estimates.

(iii) For the next example, we assume the value of the exponent n in (4), which is $\frac{3}{2}$ for the Hertz and the DMT models. Apart from n we assume no knowledge of the other tip or sample properties. In this case, (4) can be re-written as,

$$\begin{aligned}(F_{ts} - \beta)^{2/3} &= (\gamma)^{2/3}(z_s), \\ &= \psi(a_0 - p_1) + \psi(h),\end{aligned} \tag{5}$$

where we denote $\gamma^{2/3}$ by ψ, a_0 is the intermolecular distance and the separation $z_s = a_0 - p_1 - h$. From (4), it is observed that the parameter β is the minimum value of the repulsive force with respect to the tip-sample separation distances. This can be computed numerically using the available interaction force estimate $\hat{F} = \hat{\tilde{d}} - F(\hat{p}_1)$ within an error of 5%.We consistently consider a set of force estimate values corresponding to the repulsive region where the tip interacts with the sample. These force estimates are plotted against the corresponding values of $(a_0 - p_1)$. Furthermore, the change in sample height h is negligible within the force region considered. Therefore, each of the aforementioned plots results in approximately a straight line, whose slope is an estimate of ψ from (5) . The slopes may be averaged over several cycles to derive a reliable estimate for ψ. See Fig. 5(b).

(iv) Other cases that can be explored are, deriving the sample's properties for a calibration sample or a sample with known

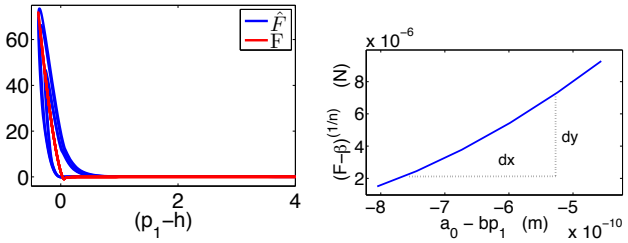

(a) (b)

Figure 5. (a) The force F corresponds to the forcing term used in our simulations for the real system and $\hat{F}$ corresponds to the estimate obtained. The phase lag in the estimate of $\tilde{d}$ (Figure 3(b)) is reflected in the plot of forces against the corresponding separations for sample (b) The plot shows the left hand side of (5) plotted against the values of $a_0 - p_1$ that are available through estimation and measurement. The slope of the plot corresponds to the value of $\psi = \gamma^{2/3}$.

sample height. This implies that an estimate of the entire z_s vector is available for use. In this case again the values of the intermolecular distance a_0 and the adhesive force parameter β can be computed from the $\hat{F}$ versus p_1 plots. To fit the values of n and γ, we plot the vector containing $\log(|F_{ts} - \beta|)$ against values of $\log(|z_s|)$. Please note that we have delineated only a few methodologies that can estimate the sample height and features, however other schemes remain to be explored. In the next section, we have validated several of our claims using simulation results.

5 CONCLUSIONS

Force regulation using the fast cantilever deflection signal allows realization of high speed scans and simultaneous estimation of the tip-sample interaction force. Consequently, it requires the support of high speed devices and we propose to implement our controller using a FPGA based module on the AFM. Low amplitude oscillations of the cantilever tip are also being considered to gather better estimates of the interaction force. It must also be noted that this paper does not take noise into consideration. We expect that a detailed characterization of noise properties will become clearer with experiments. In this paper, some examples have been explored briefly that can estimate the sample height features and physical properties using an AFM at higher speeds than existing methods owing to the high bandwidth tip-sample interaction force estimates. The interaction force estimates capture the repulsive forces experienced by the tip well even at speeds as high as $10-15\%$ of the cantilever resonance frequency. Dynamic estimates of sample properties such as stiffness can be obtained by fitting interaction models to the force estimate data. Identification of which properties can be estimated robustly from the force estimates is a part of ongoing work.

REFERENCES

[1] Binnig, G., C.F.Quate, and Gerber, C., 1986. "Atomic force microscope". *Physical Review Letters,* **56**(9), March, pp. 930–933.

[2] Fantner, G., Schitter, G., and et. al. J.H. Kindt, 2006. "Components for high speed atomic force microscopy". *Ultramicroscopy,* **106**(8), pp. 881–887.

[3] Leang, K., and Fleming, A., 2008. "High speed afm scanner: Design and drive considerations". In American Control Conference, pp. 3188–3193.

[4] Polit, S., and Dong, J., 2010. "Design of high-bandwidth high-precision flexure-based nano-positioning modules". *Journal of Manufacturing Systems*.

[5] Mohan, G., Lee, C., and Salapaka, S., 2011. "Control techniques for high-speed dynamic mode imaging in atomic force microscopes". In Proceedings of the 50th IEEE Conference on Decision and Control and European Control Conference, CDC-ECC 2011, Orlando, FL, USA, pp. 651–656.

[6] Maivald, P., Butt, H., Gould, S., Prater, C. B., Drake, B., Gurley, J., Elings, V., and Hansma, P., 1991. "Using force modulation to image surface elasticities with the atomic force microscope". *Nanotechnology,* **2**, February, pp. 103–106.

[7] Stark, M., Guckenberger, R., Stemmer, A., and Stark, R., 2005. "Estimating the transfer function of the cantilever in atomic force microscopy: A system indentification approach". *Journal of Applied Physics,* **98**, December, pp. 114904–114904–7.

[8] Giessibl, F., 2001. "A direct method to calculate tip-sample forces from frequency shifts in frequency-modulation atomic force microscopy". *Applied Physics Letters,* **78**(1), January.

[9] Yuya, P. A., Hurley, D. C., and Turner, J. A., 2009. "Contact-resonance atomic force microscopy for viscoelasticity". *Journal of Applied Physics,* **104**(7), June, pp. 074916–074916–7.

[10] Agarwal, P., and Salapaka, M. V., 2009. "Real time estimation of equivalent cantilever parameters in tapping mode atomic force microscopy". *Applied Physics Letters,* **95**(8), September, pp. 083113–083113–3.

[11] Johnson, K., Kendall, K., and Roberts, A., 1971. "Surface energy and the contact of elastic solids". *Proceedings of the Royal Society, Lond.A,* **324**(1558), September, pp. 301–313.

[12] Derjaguin, B., Muller, V., and Toporov, Y., 1975. "Effect of contact deformations on the adhesion of particles". *Journal of Colloid and Interface Science,* **53**(2), November, pp. 314–326.

[13] Pollock, H., Maugis, D., and Barquins, M., 1978. "The force of adhesion between solid surfaces in contact". *Applied Physics Letters,* **33**(9), November, pp. 798–799.